Ideal tensile strength of *B*2 transition-metal aluminides

Tianshu Li, J. W. Morris, Jr., and D. C. Chrzan
Department of Materials Science and Engineering, University of California, Berkeley, California 94720, USA
and Materials Science Division, Lawrence Berkeley National Laboratory, Berkeley, California 94720, USA
(Received 12 May 2004; published 26 August 2004)

The ideal tensile strengths of the B2-type (CsCl) transition-metal aluminides FeAl, CoAl, and NiAl have been investigated using an *ab initio* electronic structure total energy method. The three materials exhibit dissimilar mechanical behaviors under the simulated ideal tensile tests along [001], [110], and [111] directions. FeAl is weakest in tension along [001] whereas CoAl and NiAl are strongest in the same direction. The weakness of FeAl along [001] direction is attributed to the instability introduced by the filling of antibonding *d* states.

DOI: 10.1103/PhysRevB.70.054107 PACS number(s): 61.50.Lt, 62.20.Dc, 71.20.Lp

The need for high melting point, high strength and low density materials for application in the aircraft industry has driven the intensive study of transition metal aluminides FeAl and NiAl. These intermetallics, though sharing the same B2 (CsCl) structure and having similar lattice parameters, display very different cleavage behaviors. FeAl shows a strong cleavage anisotropy and cleaves along {001} in a fashion similar to that of most body-centered-cubic materials.[1,2] NiAl, in contrast, fails under tension in a more complex manner, i.e., several candidate cleavage planes (e.g., {110}, {511}, and {711}) are observed depending on the experimental conditions.[1,3,4]

From the atomistic point of view, ideally brittle fracture eventually reduces to the separating of the atomic bonds in which the ultimate bonding strength is achieved at the crack tip. Insight into the nature of the bonding with respect to the deformation renders a better understanding on the mechanical behavior of the material. Prior theoretical efforts attempt to understand the macroscopic behavioral differences of the considered B2 compounds through studies of the ionicity, charge transfer[5] and cleavage energy[6] of these materials *in their ground states*. None of these, however, has been shown to correlate strongly with observed behaviors.[5] This does not mean that correlations with the above mentioned quantities cannot be found, but rather, that the correlations, if they exist, stem from something other than the ground state properties.

Computations of ideal tensile strength explore strain ranges well beyond those governed by linear elasticity theory and, consequently, may be capable of predicting some of mechanical behaviors in these compounds. In fact, it is demonstrated here that cleavage properties deduced from a computation of ideal tensile strength correlate well with experimental observations. Further, these computations allow identification of the electronic states responsible for the observed differences in cleavage behavior.

The ideal strength is defined as the minimum stress needed to drive a defect free crystal to elastic instability, and therefore, sets the upper limit of strength that a material can never exceed.[7] For the transition-metal aluminide systems, the first calculation was made by Sob *et al.*[8,9] who studied the ideal tensile strength of NiAl pulled in [100] and [111] directions. This present work extends the work of Sob and collaborators to include a study of compounds similar to NiAl. Further, this work examines the evolution of the electronic structure along the strain path.

Calculations employed the local density approximation (LDA) to density functional theory embodied in the Vienna *ab initio* simulation package (VASP).[10] Ultra-soft pseudopotentials[11] were used. The energy cut-off was chosen to be 24 Ry. The cubic unit cell contains two atoms (one Al and one transition metal) of which one sits on the body center and the other is on the corner. For structural relaxation, a grid of $14\times14\times14$ *k*-points generated according to the Monkhorst-Pack scheme[12] was symmetry reduced and used to sample the irreducible wedge of the first Brillouin zone. When exploring the electronic structure, a finer grid ($35\times35\times35$) was chosen to generate a high quality charge density. With these choices, the total energy is converged to 1 mRy per atom. The ground state of each compound was found by minimizing the total energy as a function of the lattice parameters. The calculations predicted the equilibrium lattice constants 1.4%–3.1% smaller and the elastic constants of NiAl 2.9%–12.1% higher than experiments (Table I), suggesting a slightly over-binding, as is typical of the LDA calculations.[13]

After obtaining the equilibrium structure, a series of incremental tensile strains were applied to the crystal. To insure that the material was under a uniaxial stress state, relaxation of the structure perpendicular to the applied strain direction was performed by holding the applied strain fixed and adjusting the other two normal strain components independently until the calculated conjugate Hellmann-Feynman stresses[16] were both less than 0.1 GPa.

Under [111] uniaxial tension, a B2 crystal follows a trigonal path and its structure eventually becomes B1 (NaCl) when the engineering strain is around 0.68. Since the NaCl structure also possesses cubic symmetry, the B1 structure is also a stress-free state, implying the tensile stress must pass through at least one maximum along the strain path.[17–19] In this circumstance, the B1 structure corresponds to the local maximum of the energy curve and the inflection point gives the maximum stress, i.e., the ideal strength, under [111] tension, as shown in Fig. 1(c). FeAl and CoAl have nearly the

TABLE I. Comparison of the calculated crystal constants with the experimental data. Elastic constants are for NiAl.

	a_{FeAl}	a_{CoAl}	a_{NiAl}	C11	C12	C44
Experiments	2.91[a]	2.86[a]	2.89[a]	211.5[b]	143.2[b]	112.1[b]
Calculations	2.82	2.80	2.84	217.9	152.9	127.6
Error	−3.1%	−1.4%	−1.7%	+2.9%	+6.3%	+12.1%

[a]Experimental lattice constants from Ref. 14.
[b]Experimental elastic constants from Ref. 15.

same maximum stress, of 31 GPa, higher than the 24 GPa of NiAl. According to Orowan,[20] an extremum stress of 0.08 $E_{\langle hkl\rangle}$, where $E_{\langle hkl\rangle}$ is the elastic modulus in the $\langle hkl\rangle$ directions, is expected if one fits the stress-strain curve between the two unstressed states with a sinusoid governed by the proper elastic modulus. The calculated [111] ideal strengths in the three materials are in good agreement with Orowan's theory in this sense (for example, $\sigma_{\langle 111\rangle}=25$ GPa $=0.082\ E_{\langle 111\rangle}$ for NiAl). The ideal tensile strength in this direction is, therefore, symmetry dictated. A similar argument has been applied in previous studies[18,19,21] of the BCC$\rightarrow$FCC structural transformation along $\langle 100\rangle$ directions in BCC metals, also known as the "Bain Path."

A B2 crystal under [110] tension follows a monoclinic path on which no other high symmetry or stress-free structure is encountered. The instability is then associated with the zero stress state at infinite strain. Again, FeAl and CoAl are similar to each other in their stress strain relationships as well as their maximum stresses. NiAl, on the other hand, has a lower modulus and ideal strength. For the three materials, the ratio of the maximum stress to their respective elastic moduli is approximately 0.12.

The most interesting behavior is observed for a [001] tensile path. Maintaining the tetragonal shape as expected, the crystals undergo a B2$\rightarrow$L1$_0$ structural transformation when the stress is applied. Since L1$_0$ has reduced symmetry in comparison to B2 and no other high symmetry structure intrudes on the strain path, the instability is again expected to be determined by the "saddle point" at infinity. The calculated stress strain relation, however, shows this argument is valid only for CoAl and NiAl. FeAl, intriguingly, manifests a

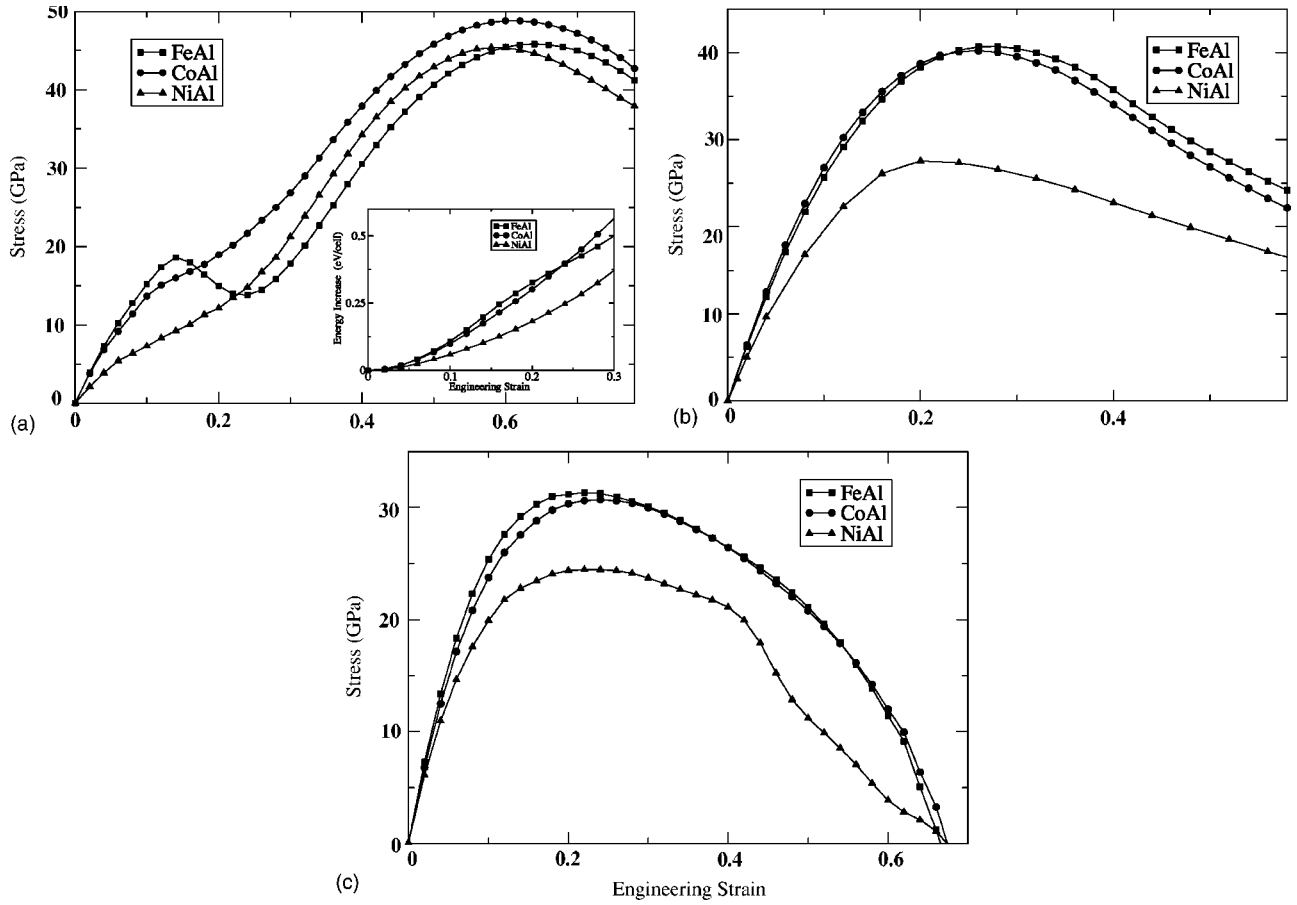

FIG. 1. Ideal tensile strength versus engineering strain for FeAl CoAl, and NiAl along (a) [001] (b)[110] (c)[111]. The energy increase per unit cell under an applied [001] tension is also included in (a).

TABLE II. Summary of the ideal tensile strength along three directions. All the stresses are in GPa.

	[001]		[110]		[111]	
	σ_m	ε_m	σ_m	ε_m	σ_m	ε_m
FeAl	19	0.14	40	0.28	31	0.22
CoAl	49	0.60	40	0.26	31	0.24
NiAl	45	0.58	27	0.20	24	0.22

small "wiggle" at a relatively low strain. Although FeAl has both the global maximum stress and the corresponding strain close to those of CoAl and NiAl, its ideal strength is defined as the first local maximum introduced by the wiggle, because the crystal has become unstable at this stress, leaving the states following unreachable. Thus, the ideal strength (19 GPa) of FeAl along the [001] direction is considerably lower than those of the other two aluminides (49 GPa for CoAl and 45 GPa for NiAl). Table II summaries the critical stress and strain for each material. Sob *et al.*[8,9] calculated the ideal tensile strength of NiAl using the full-potential linearized augmented plane wave (FLAPW) method and obtained 25 GPa in the [111] direction and 46 GPa in the [100] direction. The results obtained using the ultrasoft pseudopotentials are in good agreement with this previous study.

Clearly, no direct measurements of the ideal tensile strength of defect-free materials are available to compare with the calculations. It is also known that even in the ideal world, materials, in many cases, fail by shear rather than tension before the critical tensile strength is approached. However, it is interesting to note that experimentally FeAl shows a preference for {100} cleavage regardless of the orientation of a single crystal sample whereas the same {100} planes in CoAl and NiAl, in contrast, are unfavorable for fracture as indicated by the fact that the crack path deviates from an initial {100} notch plane in a four-point bending experiment.[1] These results, combined with our calculations, reveal the intrinsic strength differences along the ⟨001⟩ directions of the B2 transition-metal aluminides. It is important, then, to understand the electronic origins of the observed trends as this understanding may allow engineering of the cleavage properties of these alloys.

Ni, Co, and Fe all form stable B2 aluminides with similar band structures[22,23] that mainly differ from each other by the energy level of each band relative to the Fermi energy. Figure 2(a) presents the band structure along the crystalline orientations with the high symmetry of the unstrained FeAl. The bands near the Fermi level are formed mainly from the transition metal *d*-states. Three states derived from the metal *d* orbitals have T_{2g} symmetry (i.e., d_{xy}, d_{yz}, and d_{xz}) and are degenerate at Γ, lying just above the Fermi level. These bands split into d_{xy} (the sixth band) and doubly degenerate

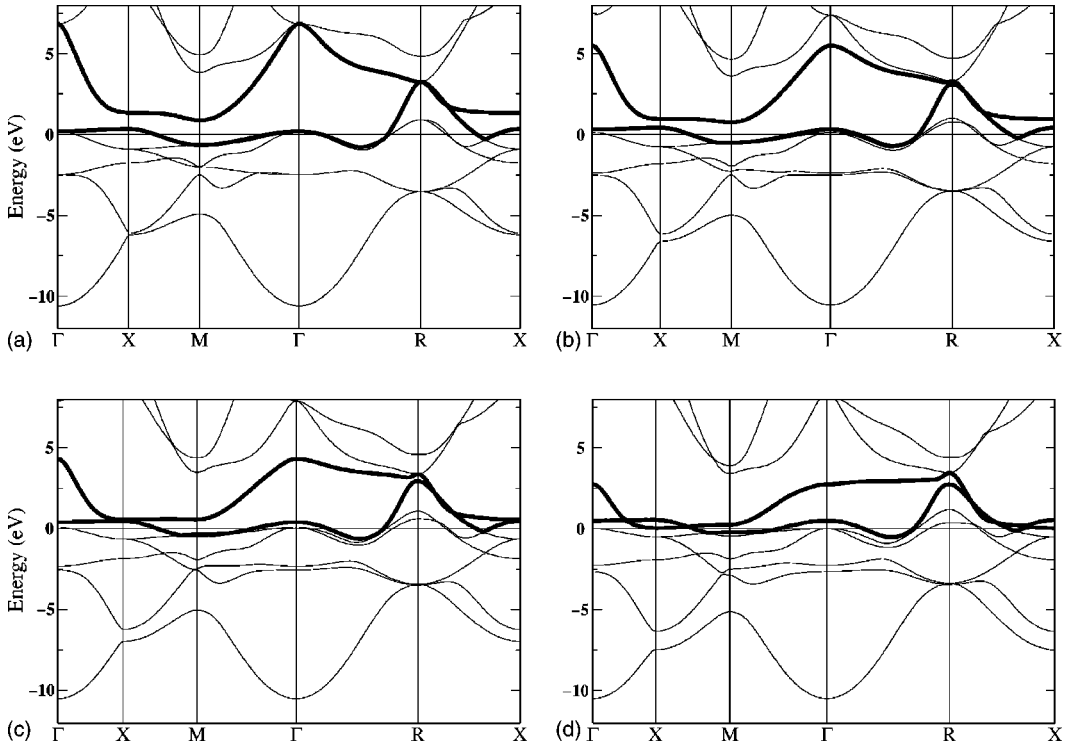

FIG. 2. Band structure of FeAl at (a) ground state, (b) $\varepsilon_{zz}=0.04$, (c) $\varepsilon_{zz}=0.08$, and (d) $\varepsilon_{zz}=0.14$. The k-point are labeled corresponding to the ground state structure for comparison. The Fermi level is set at zero energy. The sixth and seventh band (solid lines) are observed to respond oppositely under the [001] uniaxial tensile strain.

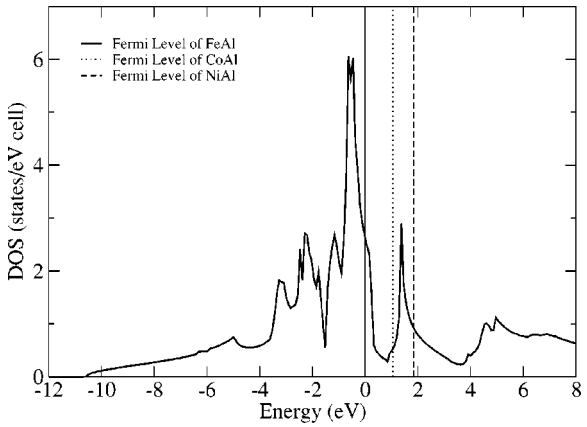

FIG. 3. Density of states in FeAl at ground state. CoAl and NiAl have similar DOS curves with their Fermi energies 1.06 eV (dotted line) and 1.85 eV (dashed line) higher than that of FeAl, respectively.

$d_{yz}+d_{xz}$ (the fourth and fifth bands) in the direction from Γ to X. The other two *d*-states, sharing E_g symmetry ($d_{x^2-y^2}$ and $d_{3z^2-r^2}$), are also degenerate at Γ with an energy approximately 2.5 eV below the Fermi level. Above the Fermi level, along X-M, the seventh band is constructed mainly from the σ bonding of the $d_{3z^2-r^2}$ orbitals from the transition metal atoms, yielding a high density of antibonding states (Fig. 3).

With a total of 11 valence electrons in the unit cell, FeAl fills its first three bands completely, the fourth and fifth bands nearly full, and leaves the sixth band slightly over half-filled. The Fermi level falls within the bonding states (Fig. 3). NiAl, in contrast, pushes its Fermi level beyond the antibonding peak by filling nearly half of the seventh band as a result of the two more valence electrons contributed by Ni. The Fermi level of CoAl resides in the "pseudo gap" which separates the bonding and antibonding states, and touches the very bottom of the seventh band near M. Filling the antibonding states would result in the energy increase of the system and hence weaken the stability of the bonding. The tendency in lattice constants decreasing from FeAl to CoAl while increasing from CoAl to NiAl is consistent with this analysis.[24]

When a uniaxial stress is applied along the [001] direction, significant changes of the energy bands near the Fermi level are observed. The three T_{2g} *d*-states are no longer degenerate and a small gap opens at Γ [Fig. 2(b)] as cubic symmetry is broken. From Γ to *X* (i.e., [001]), bands derived from d_{yz} and d_{xz} are still expected to be degenerate because the crystal follows a tetragonal path where *x* and *y* are equivalent. Near X and M, these bands rise relative to their initial levels as the strain increases. In the unstrained state, adjacent transition metal atoms (along the cube edge) on the {100} planes bind to each other via $dd\pi$ bonds involving T_{2g} orbitals. The square shape of each cubic face wherein a transition metal atom sits on each corner is thus favorable. Under tensile strain along [001], the square symmetry of (100) and (010) planes is broken leading to an energy increase for d_{yz} and d_{xz} derived bands. On the (001) plane, transition metal atoms move nearer to each other without breaking the square symmetry, pushing the d_{xy} derived band upwards as well. In contrast to the rise of *d* bands from T_{2g} symmetry upon loading, the seventh band is observed to drop in energy, mainly because the antibonding $dd\sigma$ derived states lower their energy as the interatomic distance along *z*-direction increases. This downward movement of the energy band thus contributes negatively to the total energy increase, more or less depending on how much this band has been occupied. (A similar variation of the energy band under shear stress was observed in transition-metal carbonitrides.[25]) Consequently, NiAl possesses a lower elastic modulus (105 GPa) along the [001] direction because of significant occupation of the seventh band. FeAl, on the other hand, shows a high modulus (195 GPa) as its seventh band is empty in the ground state. CoAl, with its Fermi level across the bottom of the antibonding *d*-band, has nearly the same elastic modulus (190 GPa) at the initial stage of loading as FeAl, because the negative contribution from the small portion filling of antibonding states is compensated by the complete filling of T_{2g} *d*-states. As the strain increases more antibonding states become occupied resulting in a decrease of the elastic modulus of CoAl compared to FeAl.

The d_{xy} and $d_{3z^2-r^2}$ derived bands move in opposite directions under tension and cross each other at an engineering strain of 0.08 for FeAl [Fig. 2(c)]. At the critical strain (0.14), the antibonding *d*-state touches the Fermi level, implying that electrons flow from the stable bonding state and begin to fill this antibonding *d*-state [Fig. 2(d)]. In contrast to CoAl and NiAl which have a high occupancy of bonding states near the Fermi level, FeAl has fewer valence electrons to fill the T_{2g} bonding states. Full bonding states are expected to contribute positively to the energy of the strained system. Conversely antibonding states decrease their energy with increasing strain. The energy curve of FeAl rises less rapidly than those for CoAl and NiAl beyond the critical strain. This is a direct result of filling of the previously empty antibonding *d*-band in FeAl. The inflection point introduced by this change of energy gives rise to the local maximum stress. The mechanical instability is consequently triggered by filling of the unstable electronic states before the structural instability is broken. Such antibonding $d_{3z^2-r^2}$ instability is unlikely to be dominant under [110] and [111] tension due to the different loading paths in which the bond lengths associated with the $dd\sigma$ states deviate less with respect to the unstrained antibonding states.

It is intriguing that the calculated ideal strengths for FeAl correlate well with the observed cleavage mode of the material. Although the cleavage of crystals can be complicated and detailed modeling of the crack tip region and dislocation microstructure is needed to understand fully this problem, it is tempting to correlate the ideal tensile strength with cleavage mode. The inherent anisotropy of the bonding strength in different orientations may possibly serve as the source of the fracture anisotropy. If so, the electronic origins of the cleavage properties of FeAl have been identified, and this is an important first step towards engineering, through alloying additions, the cleavage properties of FeAl.

In conclusion, the computed ideal tensile strength of FeAl differs substantially from the similar alloys NiAl and CoAl. Whereas NiAl and CoAl are strongest in [001] tension, FeAl

is weakest when pulled in the same direction. The electronic origins of the anomalous behavior of FeAl have been identified. Specifically, the crossing and filling of two *d*-bands in FeAl as a function of the applied strain state yields the computed nonmonotonic behavior for the stress vs strain curve. The ideal tensile strength study facilitates an alternative understanding of the cleavage properties of B2 transition metal aluminides. This identification may allow future engineering of the cleavage properties of FeAl.

This work was supported by the Directorate, Office of Energy Sciences, Office of Basic Energy Sciences, of the Department of Energy under Contract No. DE-AC03-76SF00098.

[1] K.-M. Chang, R. Darolia, and H. A. Lipsitt, Acta Metall. Mater. **40**, 2727 (1992).
[2] M. V. Nathal and C. T. Liu, Intermetallics **3**, 77 (1995).
[3] R. Darolia, K.-M. Chang, and J. E. Hack, Intermetallics **1**, 65 (1993).
[4] J. H. Schneibel, R. Darolia, D. F. Lahrman, and S. Schmauder, Metall. Trans. A **24**, 1363 (1993).
[5] P. A. Schultz and J. W. Davenport, J. Alloys Compd. **197**, 229 (1993).
[6] M. H. Yoo and C. L. Fu, Scr. Metall. Mater. **25**, 2345 (1991).
[7] J. W. Morris, Jr., C. R. Krenn, D. Roundy, and M. L. Cohen, in *Phase Transformations and Evolution in Materials* (TMS, Warrendale, PA, 2000), p. 187.
[8] M. Sob, L. G. Wang, and V. Vitek, Kovove Mater. **36**, 103 (1998).
[9] M. Sob, L. G. Wang, and V. Vitek, Philos. Mag. B **78**, 653 (1998).
[10] G. Kresse and J. Furthmüller, Phys. Rev. B **54**, 11169 (1996).
[11] D. Vanderbilt, Phys. Rev. B **41**, 7892 (1990).
[12] H. J. Monkhorst and J. D. Pack, Phys. Rev. B **13**, 5188 (1976).
[13] A. van de Walle and G. Ceder, Phys. Rev. B **59**, 14992 (1999).
[14] W. B. Pearson, *A Handbook of Lattice Spacings and Structures of Metals and Alloys*, Vol. 2 (Pergamon, Oxford, 1967).
[15] G. Simmons and H. Wang, *Single Crystal Elastic Constants and Calculated Aggregate Properties: A Handbook* (MIT Press, Cambridge, MA, 1971), 2nd ed.
[16] O. H. Nielsen and R. M. Martin, Phys. Rev. B **32**, 3780 (1985).
[17] P. J. Craievich, M. Weinert, J. M. Sanchez, and R. E. Watson, Phys. Rev. Lett. **72**, 3076 (1994).
[18] C. R. Krenn, D. Roundy, J. W. Morris, Jr., and M. L. Cohen, Mater. Sci. Eng., A **319**, 111 (2001).
[19] D. Roundy, C. R. Krenn, M. L. Cohen, and J. W. Morris, Jr., Philos. Mag. A **81**, 1725 (2001).
[20] E. Orowan, Rep. Prog. Phys. **12**, 185 (1949).
[21] M. Sob, L. G. Wang, and V. Vitek, Mater. Sci. Eng., A **234-236**, 1075 (1997).
[22] S.-C. Lui, J. W. Davenport, E. W. Plummer, D. M. Zehner, and G. W. Fernando, Phys. Rev. B **42**, 1582 (1990).
[23] K.-J. Kim, B. N. Harmon, and D. W. Lynch, Phys. Rev. B **43**, 1948 (1991).
[24] G. A. Botton, G. Y. Guo, W. M. Temmerman, and C. J. Humphreys, Phys. Rev. B **54**, 1682 (1996).
[25] S.-H. Jhi, J. Ihm, S. G. Louie, and M. L. Cohen, Nature (London) **399**, 132 (1999).